Journal of Alloys and Compounds 500 (2010) 46–48

Contents lists available at ScienceDirect

Journal of Alloys and Compounds

journal homepage: www.elsevier.com/locate/jallcom

Structure and electrical properties of $BiFeO_3$ thin films grown on $LaNiO_3$ electrode by chemical solution deposition

Hailei Zhang, Xinman Chen*, Tao Wang, Feifei Wang, Wangzhou Shi

Key Laboratory of Optoelectronic Material and Device, Mathematics & Science College, Shanghai Normal University, Shanghai 200234, PR China

ARTICLE INFO

Article history:
Received 19 January 2010
Received in revised form 19 March 2010
Accepted 25 March 2010
Available online 1 April 2010

PACS:
73.40.Qv
73.61.−r
74.78.Fk
77.55.Nv
81.20.Fw

Keywords:
Ferroelectrics
Surfaces and interfaces
Thin films
Sol–gel processes
Electrical transport

ABSTRACT

$BiFeO_3$ thin films were prepared on $LaNiO_3$ (LNO)-electrodized thermally oxidized silicon substrate by chemical solution deposition method. X-ray diffraction analysis revealed that the well-crystallized $BiFeO_3$ thin films were obtained with no impurity phases. The resultant $BiFeO_3$ thin films were provided with the dense and uniform surface morphology. The dielectric constant and dielectric loss at 10 kHz of $BiFeO_3$ thin film on LNO electrode were 202 and 0.057, respectively. Large double remanent polarization of 90.9 $\mu C/cm^2$ was observed. Furthermore, the trap-controlled space charge limited conduction mechanisms of the leakage current behavior of $BiFeO_3$ films on LNO electrode was suggested.

1. Introduction

In recent years, multiferroic materials coupling the different ordering phenomena have been attracting considerable attention for potential application in information storage, such as spintronics, nonvolatile memory cells and so on [1–3]. Previous investigations demonstrated that $BiFeO_3$ was one of the most actively studied multiferroic oxides with the existence of the ferroelectricity and antiferromagnetism simultaneously at room temperature due to the high Curie temperature ($T_c = 850\,^{\circ}C$) and Nèel temperature ($T_N = 370\,^{\circ}C$) [2–5]. Much interest has been aroused by realization of the large remanent polarization of epitaxial $BiFeO_3$ thin film on various substrates. However, the following applications of $BiFeO_3$ thin film in electronic devices were hampered by its serious leakage current problem related with impurity phases, boundaries, non-stoichiometry and chemical valance fluctuation of Fe ions.

To enhance the electrical properties, ferroelectric films were usually integrated on some metal oxide electrodes instead of the noble metal electrodes like Pt. Of particular interest, the $LaNiO_3$ (LNO) is a promising conducting oxide. Bao et al. reported that the formation of a coherent interface between LNO and ferroelectric films can enhance the orientation and improve the crystallinity of films, which is beneficial for the good dielectric and ferroelectric properties [6]. The larger remanent polarization and better fatigue property as well as the reduced leakage current density of the $Pb(Zr,Ti)O_3$, $(Ba,Sr)TiO_3$, $Bi_{4-x}La_xTiO_3$ films grown on LNO electrode were extensively reported before [7–10]. However, few investigations were made on $BiFeO_3$ films on LNO bottom electrode compared with $SrRuO_3$ and Pt. Meanwhile, the LNO has a perovskite structure with pseudocubic symmetry and a lattice parameter of 0.384 nm, matching well with the $BeFeO_3$ (0.396 nm) [3,7]. Therefore, the good electrical properties of $BeFeO_3$ thin films are reasonably desired. In this study, the $BiFeO_3$ thin films were deposited on LNO coated thermally oxidized silicon substrate (SiO_2/Si) by chemical solution deposition method (CSD). The structure, dielectric, ferroelectric properties as well as leakage current behavior of $BiFeO_3$ thin films were investigated.

2. Experimental

The $BiFeO_3$ thin films were prepared on thermally oxidized silicon substrates coated with LNO electrode by CSD. The $BiFeO_3$ solutions were synthesized using bismuth nitrate [$Bi(NO_3)_3 \cdot 9H_2O$] and iron nitrate [$Fe(NO_3)_3 \cdot 5H_2O$] as raw mate-

---

* Corresponding author. Tel.: +86 021 64328894; fax: +86 021 64328894.
E-mail address: xmchen@shnu.edu.cn (X. Chen).

0925-8388/$ – see front matter. Crown Copyright © 2010 Published by Elsevier B.V. All rights reserved.
doi:10.1016/j.jallcom.2010.03.192

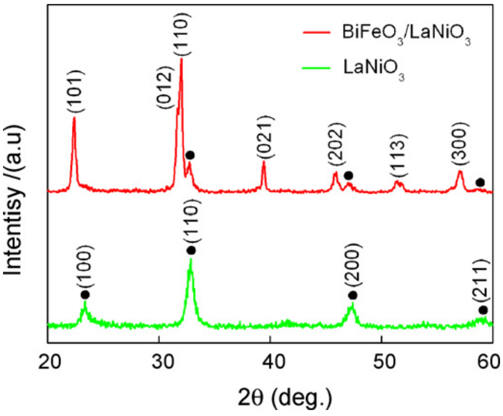

Fig. 1. XRD patterns of BiFeO$_3$ thin films deposited on LNO coated SiO$_2$/Si substrate. The patterns of BiFeO$_3$ thin films were indexed according to JCPDS card no. 20-0169. The black dots denote the peaks of LNO electrode.

rial. Bismuth nitrate and iron nitrate were dissolved into the glacial acetic acid and 2-methoxyethanol at room temperature under the constant stirring, respectively. After mixing the above solutions, a moderate amount of diethanolamine was added to obtain the smooth and dense surface. The molar ratio of Bi:Fe = 1.05:1 was identified to compensate for the Bi loss during the post-annealing process. Finally, the depositions were carried out by spin coating techniques on the LNO coated SiO$_2$/Si substrates at 3000 rpm for 15 s. Each layer was preheated at 350 °C for 5 min to remove volatile materials. The above spin coating and preheating procedures were repeated until the desired film thickness was achieved. Finally, the thin films were crystallized at 500 °C for 30 min at air ambient. The LNO thin films were also obtained by CSD, which has been described elsewhere in details [11]. Before the deposition of BiFeO$_3$ solution, the LNO thin films were crystallized at 700 °C for an hour.

The crystalline phases of BiFeO$_3$ and LNO thin films were characterized in θ–2θ mode by a Rigaku (D-MAX 2200VPC) X-ray diffractometer (XRD) with CuK$_\alpha$ radiation (λ = 0.154 nm). The surface and cross-sectional morphology was characterized by the S-4800 scanning electron microscopy (SEM, Hitachi). The SEM confirms that the thickness of BiFeO$_3$ and LNO thin films are 480 nm and 100 nm, repectively. To measure the electrical properties, Pt circular top electrodes with diameter of 0.3 mm were deposited on the surfaces of the films through a shadow mask. The dielectric constant and dielectric loss were measured using Agilent 4294a LCR meter and the ferroelectric properties were characterized by TF Analyzer 2000 System. Leakage current behaviors were analyzed by voltage scanning mode at room temperature by Keithley 236 sourcemeter.

3. Result and discussion

Fig. 1 shows the XRD patterns of BiFeO$_3$ thin films grown on LNO buffered SiO$_2$/Si substrates. The patterns of BiFeO$_3$ thin films were indexed according to JCPDS card no. 20-0169. For comparison, the XRD patterns of the bare LNO electrode with (1 1 0) preferential orientation were also shown in Fig. 1. The polycrystalline nature of BiFeO$_3$ thin films with (1 1 0) orientation is observed and all intense peaks indicate that the BiFeO$_3$ thin films annealed at 500 °C is well crystallized. Epitaxially grown BiFeO$_3$ thin films with monoclinic symmetry were reported owing to the strain between films and substrate [2]. However, according to the XRD patterns, the perovskite structure of BiFeO$_3$ thin film with rhombohedral symmetry can be confirmed, which is similar to previous reports [4,5]. Additionally, except for the patterns of LNO layers, no peak of impurity phases such as Bi$_2$Fe$_4$O$_9$ and Bi$_{46}$Fe$_2$O$_{72}$ was detected, indicating that the pure BiFeO$_3$ phase was obtained. These results suggest that the LNO thin films can serve as a good template for BiFeO$_3$ growth during the annealing process. Fig. 2 shows the typical surface morphology of BiFeO$_3$ thin films. The smooth and dense surface morphology can be observed with well-distributed fine grains. The BiFeO$_3$ and LaNiO$_3$ thin films with thickness of about 480 nm and 100 nm were confirmed by cross-sectional SEM.

Frequency-dependent dielectric constant and dielectric loss of BiFeO$_3$ thin films deposited on LNO coated SiO$_2$/Si substrates were plotted in Fig. 3. No sudden change of dielectric constant was observed in the frequency range up to 1 MHz. The dielectric constant of BiFeO$_3$ thin film decreases slightly as the frequency increases from 1 kHz, indicating that the good interfaces between films and electrodes were obtained and the ferroelectricity originates from the intrinsic polarization, not from the interface polarization [5]. The decrease of dielectric constant at high frequency was attributed to fact that the polarizations with large relaxation times cease to respond [12]. Moreover, the dielectric loss increases slowly at low frequency range, and increases when the frequency above 100 kHz, which was believed to be related with the increased contribution of dc conductivity due to the space charges near the interfaces. The dielectric constant and dielectric loss at 10 kHz were 202 and 0.045, respectively. The dielectric constant value is higher than that of BiFeO$_3$ thin films on Pt bottom electrode by chemical solution deposition, and comparable with the corresponding result obtained by PLD [13–15]. This was supposed to be related with the existence of the LNO bottom electrode, offering the nucleation sites and promoting formation of the perovskite-structure BiFeO$_3$.

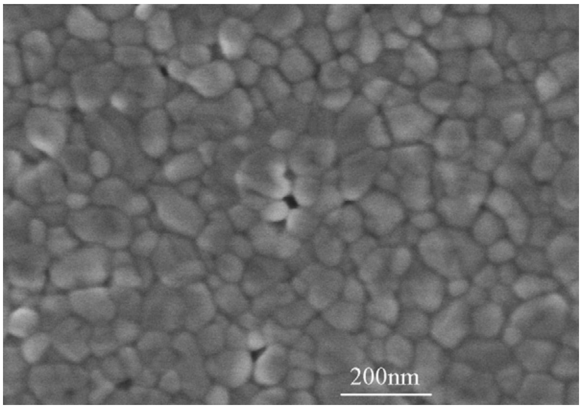

Fig. 2. SEM images surface morphology of BiFeO$_3$ thin films on LNO coated SiO$_2$/Si substrates.

The remanent polarization of BiFeO$_3$ thin films as function of applied voltage with a configuration of Pt/BiFeO$_3$/LNO/SiO$_2$/Si is shown in Fig. 4, which was measured at 1 kHz. The remanent polarization increases significantly as the applied voltage, however, the unsaturated loops can be observed, which was attributed to the large leakage current. The double remanent polarization (2P_r) and double coercive field (2E_c) of BiFeO$_3$ thin films on LNO electrode are identified to be 90.9 μC/cm^2 and 744.6 kV/cm, respectively, under the applied fields of 500 kV/cm. The 2P_r is lower than that of BiFeO$_3$ single crystals, and higher than that of BiFeO$_3$ ceramics and films on Pt, SrRuO$_3$ electrodes [13,14]. Wang et al. reported that the ferroelectricity of epitaxial BiFeO$_3$ thin films originates from the relative displacements of Bi ion and Fe–O octahedron along the (1 1 1) orientation and the larger projection polarization along the (1 1 0) orientation is observed than that of the (1 0 0) orientation. There-

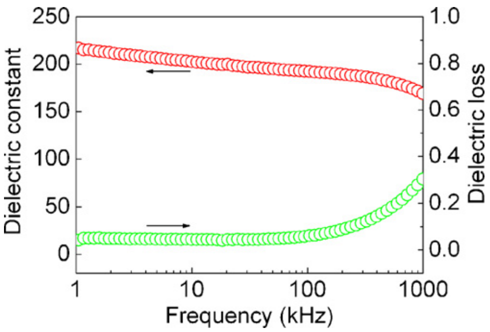

Fig. 3. Dielectric constant and dielectric loss of Pt/BiFeO$_3$/LNO films capacitor.

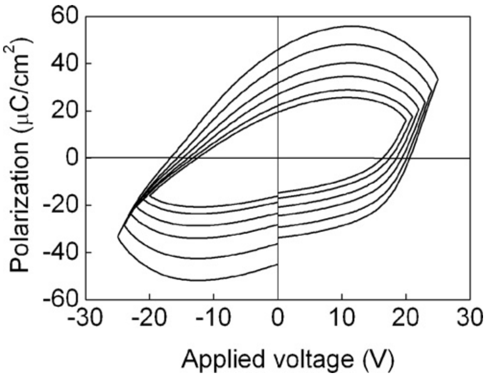

Fig. 4. The remanent polarization of $BiFeO_3$ thin films as function of applied voltage with a configuration of Pt/$BiFeO_3$/LNO/SiO_2/Si measured at room temperature.

fore, the large polarization is reasonably desired in the present work since the $BiFeO_3$ thin films show (1 1 0) preferred orientation as deposited on LNO layers.

Fig. 5a shows the typical leakage current characteristics of $BiFeO_3$ film in semi-log scale. The current–voltage (*I*–*V*) curve exhibits asymmetry in the positive and negative region. Under the applied fields of 100 kV/cm, the leakage current density of the positive region was identified to be about 1.41 μA/cm^2, which is ten times as that of negative region. This asymmetry was believed to be related with the difference of Pt and LNO electrodes. The asymmetric internal electrical fields near the film/electrode interfaces can be formed due to the accumulation of oxygen vacancies or other defects, which can compensate the applied voltage and influence the carrier injection. Meanwhile, the current density in our work is low as the $BiFeO_3$ films on Pt electrode by the chemical solution deposition, which is favorable for the large polarization at high electrical field [14]. Although large leakage current of $BiFeO_3$ thin films was generally observed, the dominant conduction mechanisms exhibit discrepancy due to the difference of granularity, grain boundaries and the film/electrode interface. The dominant Poole–Frenkel emission, trap-controlled space charge limited conduction (SCLC) mechanism and Schottky emission of $BiFeO_3$ thin films were suggested before [16,17]. To get more insight into transport behavior of carriers, the conduction mechanism of $BiFeO_3$ thin films on LNO was investigated. Fig. 5b shows *I*–*V* curve of positive branch in double-log scale. It is evident that the *I*–*V* relationship can be classified into three stages. At the low voltage region ($V < 1.2$ V), *I*–*V* curve exhibits the linear behavior, corresponding to the Ohmic conduction mechanism, which is due to the dominant thermally generated carriers inside $BiFeO_3$ thin films over the injected carriers caused by the narrower band-gap. While at higher voltage, a quadratic dependence of the current on voltage ($I \propto V^{2.3}$) was observed. And then the sharp current increase can be identified above the threshold voltage of 6.5 V with the slope reaching about 10.0 ($I \propto V^{10.0}$). The conduction behaviors can be well explained by the trap-controlled space charge limited conduction (SCLC) mechanism [18–20]. And the threshold voltage corresponds to transition voltage from the trap-unfilled region to the trap-filled region of SCLC.

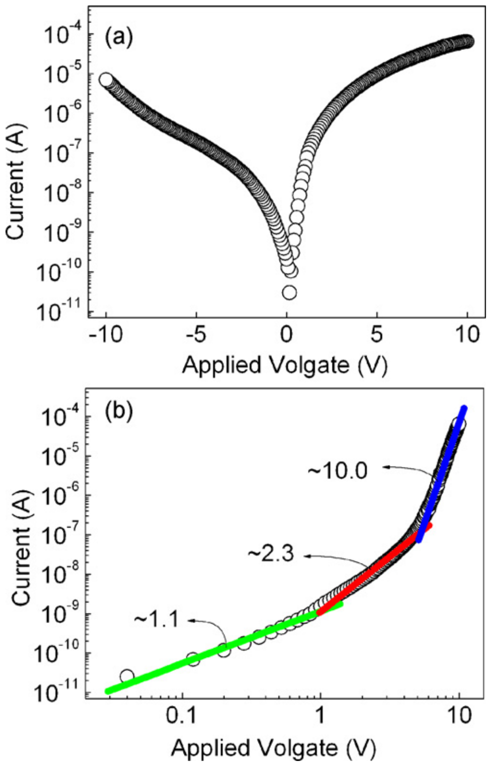

Fig. 5. Current–voltage curves of Pt/$BiFeO_3$/LNO capacitor plotted: (a) in semi-log scale, and (b) in double-log scale of positive region. The color lines denote the linearly fitting result (For interpretation of the references to color in this figure legend, the reader is referred to the web version of the article.).

In conclusion, the pure $BiFeO_3$ thin film with rhombohedral symmetry was deposited on the LNO coated thermally oxidized Si substrates by CSD. High dielectric constant and low dielectric loss of $BiFeO_3$ thin film on LNO electrode were obtained. The large double remanent polarization ($2P_r$) and double coercive field ($2E_c$) of $BiFeO_3$ films on LNO electrode are identified to be 90.9 μC/cm^2 and 744.6 kV/cm, respectively, under the applied fields of 500 kV/cm. Meanwhile, the leakage current conduction behavior of $BiFeO_3$ films on LNO electrode was dominated by the space charge limited conduction mechanisms.

Acknowledgment

The authors gratefully acknowledge support from the Leading Academic Discipline Project of Shanghai Normal University (No. DZL712).

References

[1] R. Ramesh, N.A. Spaldin, Nat. Mater. 6 (2007) 21–29.
[2] J. Wang, J.B. Neaton, H. Zheng, V. Nagarajan, S.B. Ogale, B. Liu, D. Viehland, V. Vaithyanathan, D.G. Schlom, U.V. Waghmare, N.A. Spaldin, K.M. Rabe, M. Wuttig, R. Ramesh, Science 299 (2003) 1719–1722.
[3] J. Wang, H. Zheng, Z. Ma, S. Prasertchoung, M. Wuttig, R. Droopad, J. Yu, K. Eisenbeiser, R. Ramesh, Appl. Phys. Lett. 85 (2004) 2574.
[4] C.H. Yang, J. Seidel, S.Y. Kim, P.B. Rossen, P. Yu, M. Gajek, Y.H. Chu, L.W. Martin, M.B. Holcom, Q. He, P. Maksymovych, N. Balke, S.V. Kalinin, A.P. Baddorf, S.R. Basu, M.L. Scullin, R. Ramesh, Nat. Mater. 8 (2009) 485–493.
[5] Z. Liu, H. Liu, G. Du, J. Zhang, K. Yao, J. Appl. Phys. 100 (2006) 044110.
[6] D. Bao, X. Yao, N. Wakiya, K. Shinozaki, N. Mizutani, J. Phys. D: Appl. Phys. 36 (2003) 1217–1221.
[7] D. Bao, K. Ruan, T. Liang, J. Sol–Gel Sci. Technol. 42 (2007) 353–356.
[8] M. Jain, B.S. Kang, O.X. Jia, Appl. Phys. Lett. 89 (2006) 242903.
[9] K.H. Yoon, J.H. Sohn, B.D. Lee, D.H. Kang, Appl. Phys. Lett. 81 (2002) 5012.
[10] A.Z. Simões, A. Ries, F.M. Filho, C.S. Riccardi, J.A. Varela, E. Longo, Appl. Phys. Lett. 85 (2004) 5962.
[11] G.H. Wu, K.B. Ruan, T. Liang, X.M. Chen, D.H. Bao, Thin Solid Films 517 (2009) 1563–1566.
[12] G.Z. Liu, G. Wang, C.C. Wang, J. Qiu, M. He, J. Xing, K.J. Jin, H.B. Lu, G.Z. Yang, Appl. Phys. Lett. 92 (2008) 122903.
[13] D. Lebeugle, D. Colson, A. Forget, M. Viret, Appl. Phys. Lett. 91 (2007) 022907.
[14] S.K. Singh, H. Ishiwara, K. Maruyama, J. Appl. Phys. 100 (2006) 064102.
[15] K.Y. Yun, D. Ricinschi, T.T. Kanashima, M. Okuyama, Appl. Phys. Lett. 89 (2006) 192902.
[16] G.W. Pabst, L.W. Martin, Y.H. Chu, R. Ramesh, Appl. Phys. Lett. 90 (2007) 072902.
[17] Z. Zhong, H. Ishiwara, Appl. Phys. Lett. 95 (2009) 112902.
[18] X. Chen, G. Wu, D. Bao, Appl. Phys. Lett. 93 (2008) 093501.
[19] X. Chen, G. Wu, W. Liu, P. Jiang, D. Bao, Appl. Phys. Lett. 94 (2009) 033501.
[20] A. Odagawa, H. Sato, I.H. Inoue, H. Akoh, M. Kawasaki, Y. Tokura, Phys. Rev. B 70 (2004) 224403.